Failure probability estimation of natural gas pipelines due to hydrogen embrittlement using an improved fuzzy fault tree approach

Qin, Guojin; Li, Ruiling; Yang, Ming; Wang, Bohong; Ni, Pingan; Wang, Yihuan

DOI
10.1016/j.jclepro.2024.141601

Publication date
2024

Document Version
Final published version

Published in
Journal of Cleaner Production

Journal of Cleaner Production 448 (2024) 141601

Contents lists available at ScienceDirect

Journal of Cleaner Production

journal homepage: www.elsevier.com/locate/jclepro

Failure probability estimation of natural gas pipelines due to hydrogen embrittlement using an improved fuzzy fault tree approach

Guojin Qin[a,b], Ruiling Li[a], Ming Yang[c,d,e], Bohong Wang[f], Pingan Ni[g], Yihuan Wang[a,b,*]

[a] School of Civil Engineering and Geomatics, Southwest Petroleum University, Chengdu, Sichuan, 610500, China
[b] School of Ocean and Civil Engineering, Shanghai Jiao Tong University, Shanghai, 200240, China
[c] Safety and Security Science Section, Faculty of Technology, Policy, and Management, Delft University of Technology, Jaffalaan 5, 2628 BX, Delft, the Netherlands
[d] Centre of Hydrogen Energy, Institute of Future Energy, Universiti Teknologi Malaysia, 81310, Johor Bahru, Johor, Malaysia
[e] Australian Maritime College, University of Tasmania, Launceston, TAS, 7250, Australia
[f] National & Local Joint Engineering Research Center of Harbor Oil & Gas Storage and Transportation Technology/Zhejiang Key Laboratory of Petrochemical Environmental Pollution Control, Zhejiang Ocean University, No.1 Haida South Road, Zhoushan, 316022, China
[g] College of Architecture, Xi'an University of Architecture and Technology, Xi'an, 710055, China

A R T I C L E I N F O

Handling Editor: Cecilia Maria Villas Bôas de Almeida

Keywords:
Blended hydrogen natural gas pipelines
Failure probability estimation
Fuzzy fault tree analysis
Hydrogen embrittlement
Hydrogen-induced cracking
Hydrogen blistering

A B S T R A C T

The estimation of failure probability is challenging in hydrogen embrittlement in steel pipelines due to the complexity of the synergistic effect of multiple factors. The present study proposed a hybrid methodology to estimate the failure probability of steel pipelines due to hydrogen embrittlement. The methodology integrates the fault tree analysis with a fuzzy comprehensive evaluation. Fault tree analysis captures the logical relationships between influencing indicators to develop a new assessment model of hydrogen embrittlement in steel pipelines. An improved fuzzy fault tree analysis method was proposed to process aleatoric and epistemic uncertainties to estimate the probability of each basic event due to the difficulty in obtaining the actual probabilities. The failure probability of blended hydrogen natural gas pipelines was estimated by considering the correlation of events. A case study demonstrated the applicability of the proposed method. Maintenance measures can be implemented according to the evaluation results to ensure pipeline safety.

1. Introduction

Fossil energy sources is a key driver of greenhouse gas emissions, resulting in the global climate change and environmental degradation (Qin et al., 2023; Li et al., 2022a, b). In response to this pressing concern, pursuing a net-zero emissions future has given rise to the prominence of hydrogen energy as a pivotal player in the landscape of energy transition (Wang et al., 2023). Hydrogen energy is a critical productivity in this transition, offering a paradigm shift towards a cleaner, greener, and more environmentally sustainable energy alternative (Dutta, 2014). Positioned as a cornerstone in the blueprint for an ideal future energy framework, hydrogen has the potential to revolutionize the energy consumption structure, mitigating the adverse effects of traditional fossil fuel reliance (Zhao et al., 2023). However, amidst this optimistic vision, a current bottleneck looms large—large-scale hydrogen transportation poses a significant challenge, hindering the integration of hydrogen energy into mainstream energy systems (Shah et al., 2021; Cui and Aziz, 2023). Tackling this hurdle is crucial for realizing the full potential of hydrogen as a transformative force in the energy landscape. Overcoming transportation challenges will pave the way for widespread adoption and amplify the impact of hydrogen energy in ushering in a sustainable and eco-friendly era of energy consumption (Cheng and Cheng, 2023).

The pressured steel pipeline has become an essential carrier for hydrogen energy transportation due to its economical and efficient (Cheng and Cheng, 2023). However, constructing new hydrogen pipelines does not seem feasible in countries with a large number of pipelines due to issues such as new materials, new transportation technologies, and land occupation. To address the challenge of expensive infrastructure development of hydrogen pipelines, a hybrid transportation approach is employed by blending hydrogen into existing natural gas pipelines at specific volume concentrations (Pluvinage et al., 2019; Elaoud and Hadj-Taïeb, 2008). Nevertheless, such a blending process introduces hydrogen atoms by decomposing hydrogen molecules under

* Corresponding author. School of Civil Engineering and Geomatics, Southwest Petroleum University, Chengdu, Sichuan, 610500, China.
E-mail address: yihuan.wang@swpu.edu.cn (Y. Wang).

https://doi.org/10.1016/j.jclepro.2024.141601
Received 6 December 2023; Received in revised form 12 February 2024; Accepted 29 February 2024
Available online 5 March 2024

piping conditions, leading to hydrogen embrittlement (HE), such as hydrogen-induced cracking (HIC) and hydrogen blistering (HB). The previous works have investigated the influencing factors of the HE in the pipelines mainly carried out from the following aspects: thermodynamic conditions of hydrogen atom generation (Ohaeri et al., 2018; Sun et al., 2022; Sun and Cheng, 2021a,b), permeation (Wu et al., 2022; Huang et al., 2017; Ge et al., 2020) and diffusion behavior (Ranjbar et al., 2021; Liu et al., 2009; Guo et al., 2023a,b; Zhang and Cheng, 2023) of hydrogen atoms and the failure mechanisms (Mao et al., 2022; Molavitabrizi et al., 2022; Huang et al., 2023). The failure risk of natural gas pipelines is heightened due to HE (Erdener et al., 2023), resulting in energy losses (hydrogen and natural gas), carbon emissions, and potential casualties. Hence, prioritizing the safety of blended hydrogen natural gas (BHNG) pipelines is an urgent requirement (Li et al., 2023).

Integrity management provides a lean management process for energy pipelines involving detection, evaluation, decision-making, and maintenance (Khan et al., 2021; Ali et al., 2022). The procedures are risk-based, proactive measures designed to mitigate risks and prevent accidents, primarily encompassing risk analysis and control (Chen et al., 2021). Pipeline risk is determined by multiplying the failure probability of the pipeline and its corresponding consequences. Assessing the failure probability is a critical step in risk analysis. Exploring the influencing indicators is the primary work for such assessment. The effects of factors such as gas pressure (Jiang et al., 2021; Mohtadi-Bonab, 2022; Meng et al., 2017), impurity gases (Nguyen et al., 2020; Martin and Sofronis, 2022; Zhou et al., 2007; Silva et al., 2021), service environment (Li et al., 2022a, b; Yen and Huang, 2003), composition of pipeline steel (Li et al., 2018; Yadav et al., 2022; Zhou et al., 2019; Pourazizi et al., 2021; Lang et al., 2023), micro-defects or surface defects (Han et al., 2019; Dunne et al., 2016; Ren et al., 2008; Zhang et al., 2019; Zhang and Cheng, 2023), and stress conditions (Song et al., 2020; Xu et al., 2022; Kim et al., 2021) on HIC and HB have been examined to demonstrate the occurrence of HE attributing to synergistic effects of many factors. Multivariate modeling methods have been extensively examined, including approaches based on historical failure data (Shan et al., 2018; Dundulis et al., 2016; Arena et al., 2022), Bayesian network (BN) modeling (Dahire et al., 2018; Hong et al., 2023; Li et al., 2022a, b; Adumene et al., 2020, 2021a, 2021b), hybrid models (Huang et al., 2023; Zhang et al., 2018; Feng et al., 2020), and reliability analysis (Wang et al., 2021; Yu et al., 2021; Wang et al., 2022a, b; Wang et al., 2022c). However, the existing studies have not proposed an effective indicator system to comprehensively reflect the influencing factors affecting the occurrence of HE. In addition, the above approach requires sufficient data for further quantitative analyses. While hydrogen blending technology is gaining widely attention, the actual deployment of BHNG pipeline networks is still in its infancy (Jia et al., 2023). As a result, failure and operation data for BHNG pipelines are difficult to obtain. It can be concluded that, it is impractical to accurately estimate the failure probability of BHNG pipelines using above methods. Fault tree analysis (FTA) can model multiple factors into an integrated model (Jianxing et al., 2019; Badida et al., 2019; Cheliyan and Bhattacharyya, 2018). Fuzzy fault tree analysis (FFTA) has been proven to provide practical solutions to these challenges by incorporating subjective uncertainties treatment into risk assessment. When quantitative data is limited, FFTA can effectively enable the integration of subjective judgment and qualitative expert knowledge within the risk assessment process. In previous work, for example, Girgin and Krausmann (2013) proposed using fuzzy set theory (FST) to address the issue of limited data availability by adopting expert judgments. However, the work ignores correlations or dependencies between events and the subjectivity of expert judgment that may affect the accuracy of risk assessment.

In this work, an indicator system was developed regarding HE, which was mapped into a new FTA model. An improved fuzzy fault tree analysis method (IFFTA) was proposed for estimating the failure probability of BHNG pipelines. The IFFTA method aims to address insufficient historical data and high uncertainties to improve assessment accuracy. A hybrid fuzzy set theory with semantic evaluation methods is used to estimate the failure probability of the BEs. Using the incomplete intuitionistic fuzzy preference relations to determine the expert weights improves the accuracy of expert judgment. The failure probability was calculated based on considering the correlation between events in the FTA model. The applicability of the proposed method was demonstrated by a case study. The influencing factors of significant contributions were analyzed to propose risk mitigation measures concerning the pipeline structure and external measures. This work has significant implications for pipeline operators and provides valuable insights into the suitability of natural gas pipelines for hydrogen transportation.

2. Background

This section will describe the mechanism of HE. The indicator system was developed related to HE. Furthermore, some basic concepts and terminology of fault tree analysis will be introduced.

2.1. Failure mechanisms of steel pipelines subjected to HE

Hydrogen-induced degradation refers to the failure of metals caused by the interaction between hydrogen atoms and the metal matrix. In the case of steel pipelines, HE can manifest in various ways, such as HIC and HB. Fig. 1 shows the process from hydrogen atom generation to HE. Under high-pressure hydrogen environments, hydrogen molecules decompose into hydrogen atoms under piping conditions (Cheng, 2023). Fig. 2 visually depicts the deterioration resulting from hydrogen atoms penetrating steel pipes. Hydrogen atoms are generated by dissociating H_2 molecules and permeating the pipeline steel (Sun and Cheng, 2021a, b). Once inside the metal, these hydrogen atoms can gather at localized sites, forming gaseous hydrogen molecules through the interaction between hydrogen atoms. The accumulation of these molecules leads to a significant increase in local pressure. When hydrogen bubbles accumulate on the inner surface of the metal, and the metal retains its ductility, bulging or blistering, known as HB, can occur on the outer surface. This process accelerates the degradation of pipeline properties, ultimately reducing the service life of the pipeline (Han et al., 2019). Moreover, when hydrogen atoms accumulate at the tips of pre-existing defects or microcracks, the metal bonding strength decreases, and the applied tensile stress is more likely to exceed the interatomic bonding force,

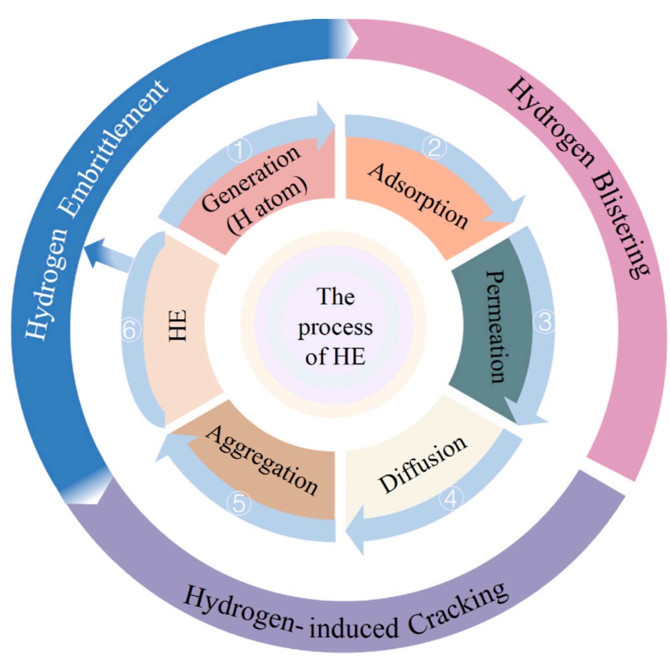

Fig. 1. The process of hydrogen embrittlement.

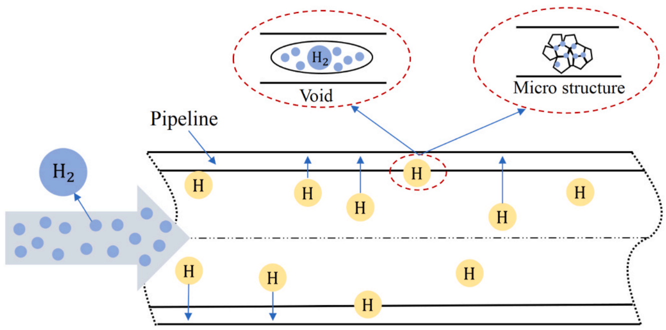

Fig. 2. Mechanism of hydrogen-induced degradation of steel pipelines.

which is more likely to lead to crack initiation or promote crack propagation, i.e., HIC (Ranjbar et al., 2021). Both HIC and HB are capable of causing BHNG pipeline failure.

2.2. Indices and indicators

An indicator system regarding HE was developed through the literature review and report analysis, as shown in Table 1. The first-class indices were HIC and HB. Eight indices related to HIC or HB are identified as second-class indices. The remaining indicators (Third- or fourth-class) are the influencing factors contributing to the second-class indices.

(1) Gas pressure

Elevated hydrogen gas pressure or a high hydrogen blending ratio within the pipeline can result in increased internal pressure, reducing the fracture toughness of the pipeline steel. This decrease in fracture toughness enhances the propagation of cracks and facilitates HIC

Table 1
The proposed indicator system regarding HE in steel pipelines.

First class	Second class	Third class	Fourth class
Hydrogen blistering	Blistering initiation	Inclusions	Al Mg oxide Al–Mg–Ca oxide
		Hydrogen concentration	
	Blistering propagation	Tempering temperature	–
		Incoherent NbC	–
Hydrogen induced cracking	Environmental factors	Gas pressure	Hydrogen blending ratio
		Impurity gas	H_2S H_2O
		Service environment	Temperature pH value
	Material factors	Ferrite-pearlite phases	–
		Pipeline steel composition	S element P element Mn element Si element Al element Al_2O_3 MgO CaO SiO_2 MnS CaS
		Defects	Dents Cracks Corrosion defects Manufacturing defects
	Stress factors	External stress	Pre-strain Axial tensile stress
		Residual stress	–

(Ranjbar et al., 2021; Pourazizi et al., 2021).

(2) Impurity gases

Impurity gases, such as H_2S, have been found to promote HE (Martin and Sofronis, 2022). When H_2S is present, it undergoes adsorption and dissociation within the pipeline, generating hydrogen atoms that permeate into the pipeline steel. These hydrogen atoms tend to accumulate at defects and microcrack tips, leading to the embrittlement of the pipeline steel (Ranjbar et al., 2021).

(3) Service environment

The service environment of the pipeline, including temperature and pH conditions, can significantly influence its performance. Elevated service temperatures can have detrimental effects on the lifespan and integrity of the pipe material. Higher temperatures can accelerate hydrogen atom diffusion and exacerbate HE in the pipeline steel. Similarly, the pH level of the environment plays a crucial role. A lower pH value, indicating a more acidic environment, can promote the enhanced diffusion of hydrogen atoms into the material. This increased diffusion further raises the susceptibility of pipeline steel to HE (Han et al., 2019).

(4) Composition of pipeline steel

Pipeline steel is commonly characterized by the presence of impurities resulting from the manufacturing process. These impurities include elements such as sulfur (S), phosphorus (P), and silicon (Si), as well as impurity oxides like silicon dioxide (SiO_2), aluminum oxide (Al_2O_3), and magnesium oxide (MgO). Additionally, compounds like manganese sulfide (MnS) and calcium sulfide (CaS) may be present in the steel. The high concentration of these impurities can have detrimental effects on the fracture toughness of the pipeline steel. These impurities can contribute to the promotion of HIC, decreasing the material's fracture toughness (Ohaeri et al., 2018; Han et al., 2019; Song et al., 2020).

(5) Defects

Aging natural gas pipelines can develop defects such as cracks, corrosion defects, and mechanical dents due to natural disasters, corrosive environments or human destruction. These defects are inevitable consequences of the pipeline's service life. When these defects are present, they have the potential to capture specific concentrations of hydrogen atoms. Local walls at these defects exhibit stronger adsorption energy than the intact wall, especially under high operating pressure (Guo et al., 2023a,b). This increased adsorption energy makes these localized areas more susceptible to HIC (Han et al., 2019). In other words, the presence of defects creates sites where hydrogen atoms have a higher affinity to accumulate and interact with the pipeline material, leading to an increased likelihood of HIC occurrence.

(6)Stress

The presence of stress on the metal surface can cause an increase in surface energy. In turn, it enhances the adsorption of hydrogen atoms onto the metal surface and hinders their desorption. Such a phenomenon results in a higher concentration of hydrogen atoms beneath the surface of the metal. Consequently, the HE susceptibility of the pipeline is significantly increased. Various factors can contribute to the occurrence of stress on the pipeline surface. For instance, soil movement can generate axial tensile stress, and internal pressure can cause circumferential stress on the pipeline. At the same time, pre-strain (prior deformation) can also impact the sensitivity to HE. These factors influence the mechanical state of the pipeline and its response to the presence of hydrogen, potentially exacerbating the effects of HE (Zhou et al., 2019; Cheng, 2022; Jiang et al., 2021).

(7) Blistering initiation

Certain impurities present in the pipeline steel, such as Al–Mg oxides and Al–Mg–Ca oxides, have been found to promote the occurrence of hydrogen blistering (Ranjbar et al., 2021; Yadav et al., 2022; Xu et al., 2022). Blistering is caused by the cavities formed under pressure through poor adhesion between the matrix and the inclusion of pipeline steel when the metal has good ductility. Such impurities contribute to the formation and growth of hydrogen gas blistering on the outer surface of the pipeline steel when hydrogen atoms combine and aggregate.

(8) Blistering propagation

Excessively high tempering temperatures or the presence of large-sized incoherent NbC precipitates have been identified as factors that can promote the propagation of hydrogen bubbles within the pipeline steel, thereby posing a potential risk of damage (Pourazizi et al., 2021; Xu et al., 2022). When pipeline steel undergoes tempering at excessively high temperatures, it can form large-sized incoherent NbC precipitates. The bonding force is weak at the sedimentary matrix to capture the hydrogen atoms more likely, and dislocations generally accumulate around large deposits, making the stress field more pronounced. Therefore, large NbC precipitates can directly lead to blister phenomenon. The presence of these hydrogen bubbles can lead to localized weakening of the material and increase the susceptibility to HB.

2.3. *Fault tree analysis*

FTA is a deductive, top-down methodology utilized for analyzing the least expected state of a system. It employs Boolean logic to integrate a sequence of lower-level events (Badida et al., 2019). The approach commences with identifying the top least expected event and then traces back the potential scenarios that can lead to the occurrence of the accident. In a fault tree, the top event (TE), intermediate events (IE), and basic events (BEs) are interconnected using logic gates. These gates demonstrate the relationships among the input events required to manifest a fault at the gate's output. AND gates are used to combine input events with the condition that all input events must coexist concurrently for the output to materialize. OR gates also combine input events. However, the occurrence of any one input event is adequate to trigger the output (Yazdi et al., 2023). In this work, "Blended hydrogen natural gas pipeline failure" is considered as the TE. It is worth noting that the occurrence of either HIC or HB can result in the BHNG pipeline failure. Therefore, an "OR gate" is employed to associate these two IEs.

According to the developed indicators system, many causes can also lead to HIC or HB. Since any of them could cause HIC or HB, these can be connected by an "OR gate". In addition, if a combination causes HIC or HB, these must be connected by an "AND gate". The sub-events are treated as new IEs and replaced with refined events. The fault tree is refined until all branches end with basic or undeveloped events to construct the FTA model of the "Blended hydrogen natural gas pipeline failure" entirely.

3. The proposed methodology

The proposed method of this work is presented in Fig. 3. Firstly, a FTA model is constructed by searching for literature and data. Secondly, the probability of BEs is calculated using a hybrid approach of semantic evaluation based on incomplete intuitionistic fuzzy preference relations and FST. Then, calculate the correlation between events through relevant probability models. Ultimately, the use of the ascending method calculates the failure probability of the TE. Ultimately, using risk acceptance criteria help maintenance decision-making.

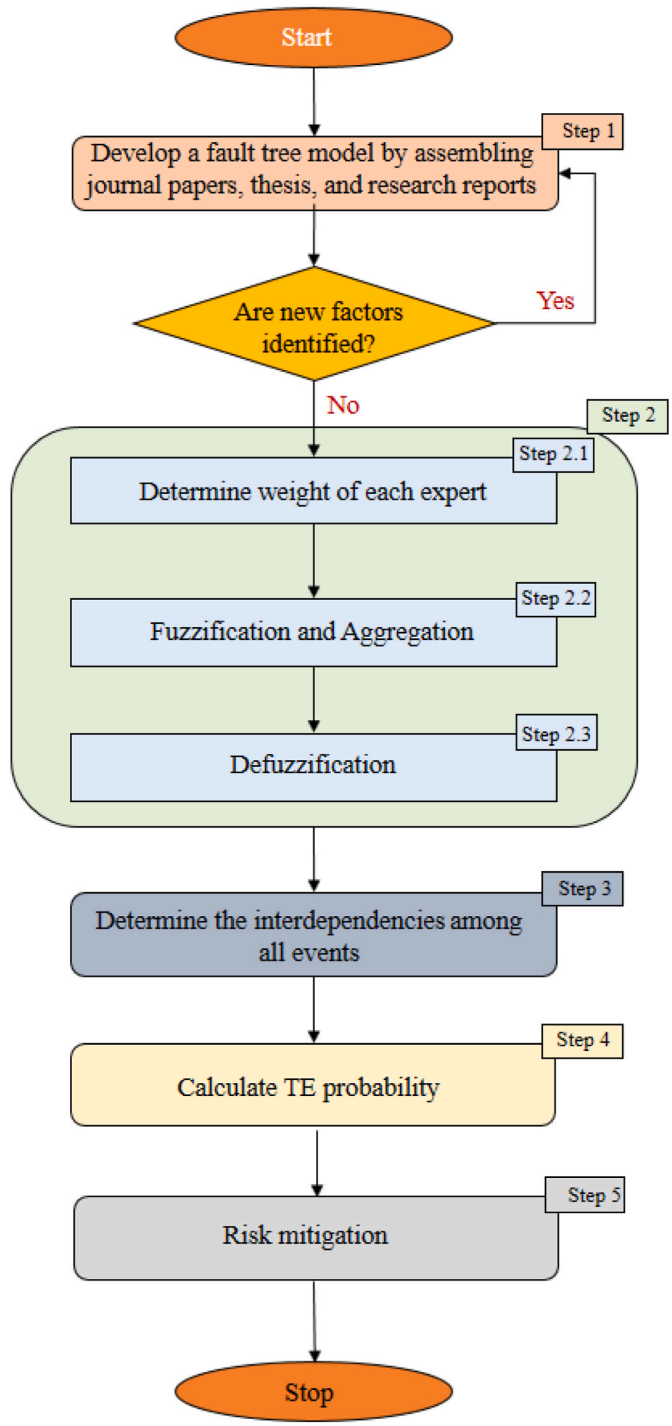

Fig. 3. The proposed method.

3.1. *Step 1: development of an FTA model for BHNG pipelines*

In analyzing accidents and potential hazards in the system, the TE considered in this work is "Blended hydrogen natural gas pipeline failure". Various interactions between indicators were represented by logical relationships. BHNG pipeline fails due to various contributing factors, including HE and conventional failure factors of natural gas pipelines. Since HE can independently lead to pipeline failure, a FTA model is constructed for BHNG pipelines by linking HE with conventional influence factors using an "OR gate." This work focuses on two typical failure modes of HE, i.e., HIC and HB. The FTA is implemented to identify the influencing factors associated with HB and HIC, identifying various basic events (BEs) representing different failure scenarios. A FTA model was constructed based on different failure modes of HE in pipelines. Fig. 4 illustrates the developed FTA model for HE, excluding the influence of pipe weld zones. Table 2 lists the BEs included in the FTA model for HE, 30 BEs in total.

3.2. Step 2: estimation of BEs probabilities

Historical data has been recognized as a practical approach to quantifying the failure probability of BEs (Khan et al., 2021). However, in cases where data is limited, conducting statistical analysis becomes challenging. To address this issue, a hybrid approach that combines semantic judgment based on incomplete intuitionistic fuzzy preference relations and FST is employed in this work to capture the aleatoric uncertainties associated with the occurrence of BEs and quantify their failure probabilities. Experts are assembled to estimate the likelihood of BE occurrences, and their collective judgments are considered. The experts are invited to assess the probability of each BE based on their expertise, knowledge and existing process reports, site conditions, and media conditions. Expert weights are applied to process the epistemic uncertainties associated with expert judgments, considering each expert's level of confidence and knowledge. In semantic evaluation methods, events are typically classified into different degrees of likelihood, as shown in Fig. 5. However, only using these semantic values cannot quantify the failure probability. FST is employed to transform the semantic values provided by the experts into possibility values, allowing for a more precise assessment of the failure probabilities. By combining semantic evaluation and FST, the hybrid approach enables the integration of expert judgments and linguistic expressions into a quantitative framework, providing a more robust estimation of the probabilities of the BEs in the FTA model for HE.

3.2.1. Step 2.1: determination of expert weights

In group decision-making, the weight of each expert is determined based on their attributes and qualifications (Wang et al., 2022a, b). In this work, the attributes considered for weight allocation are professional position, experience, and educational background. These attributes are assigned weights on a scale of 1–5, reflecting their relative importance in decision-making. Table 3 shows the weight allocation for the attributes. Using incomplete intuitionistic fuzzy preference relations, the group decision-making process considers the weights assigned to each expert based on their characteristics. These weights reflect the expertise and qualifications of the experts and help in determining the level of influence each expert has on the final decision-making process, which helps to reduce the subjectivity of expert evaluations.

Table 2
List of BEs in FTA model for HE.

BE	Description	BE	Description
X_1	High content of Al Mg oxide	X_{16}	High content of Si element
X_2	High content of Al–Mg–Ca oxide	X_{17}	High content of Al element
X_3	High hydrogen concentration	X_{18}	High content of Al_2O_3
X_4	High tempering temperature	X_{19}	High content of MgO
X_5	Large size of incoherent NbC	X_{20}	High content of CaO
X_6	High gas pressure	X_{21}	High content of SiO_2
X_7	High hydrogen blending ratio	X_{22}	High content of MnS
X_8	High content of H_2S	X_{23}	High content of CaS
X_9	High content of H_2O	X_{24}	Existence of dents
X_{10}	High temperature	X_{25}	Existence of cracks
X_{11}	Low pH value	X_{26}	Existence of corrosion defects
X_{12}	Existence of ferrite-pearlite phases	X_{27}	Existence of manufacturing defects
X_{13}	High content of S element	X_{28}	High pre-strain
X_{14}	High content of P element	X_{29}	High axial tensile stress
X_{15}	High content of Mn element	X_{30}	Existence of residual stress

Let $V = \{V_1, V_2, \cdots V_n\}$ be a discrete set of alternatives, and $P = \{p_1, p_2, \cdots, p_m\}$ be the set of experts. Each expert ($p_m \in P$) assigns a complex intuitionistic fuzzy preference value to every alternative solution, forming a comprehensive intuitionistic fuzzy preference relationship $\Re^{(k)} = (\widetilde{h}_{ij}^{(k)})$. The following three definitions introduce fundamental concepts associated with complex fuzzy sets, intuitionistic fuzzy sets, and fuzzy preference relations (Wang et al., 2022a, b).

D1: Let $\mathrm{H} = \{\langle \mathrm{x}, \alpha_H(\mathrm{x})\rangle : \mathrm{x} \in \mathrm{U}\}$ denote a complex fuzzy set on the universe U, where the membership function $\alpha_H(\mathrm{x})$ of complex values is presented as Eq. (1):

$$\alpha_H(\mathrm{x}) = r_H(\mathrm{x}) \bullet e^{\iota \omega_H(\mathrm{x})} \quad \iota = \sqrt{-1} \tag{1}$$

where both $r_H(\mathrm{x})$ and $\omega_H(\mathrm{x})$ are real numbers and within $[0, 1]$.

D2: Let $\widetilde{H}$ denote a complex intuitionistic fuzzy set on U, which is characterized by the membership function $\alpha_{\widetilde{H}}(\mathrm{x})$ and non-membership function $\beta_{\widetilde{H}}(\mathrm{x})$. Any $\mathrm{x} \in \mathrm{U}$ in $\widetilde{H}$ is assigned degree values according to the assigned levels of the membership and non-membership functions.

According to *D2*, the real numbers $\alpha_{\widetilde{H}}(\mathrm{x})$, $\beta_{\widetilde{H}}(\mathrm{x})$, and their sum can be located within a circle in the complex plane. For the form of the membership function, it is presented as Eq. (2):

$$\alpha_{\widetilde{H}}(\mathrm{x}) = r_{\widetilde{H}}(\mathrm{x}) \bullet e^{\iota 2\pi(\omega_{\alpha\widetilde{H}}(\mathrm{x}))} \tag{2}$$

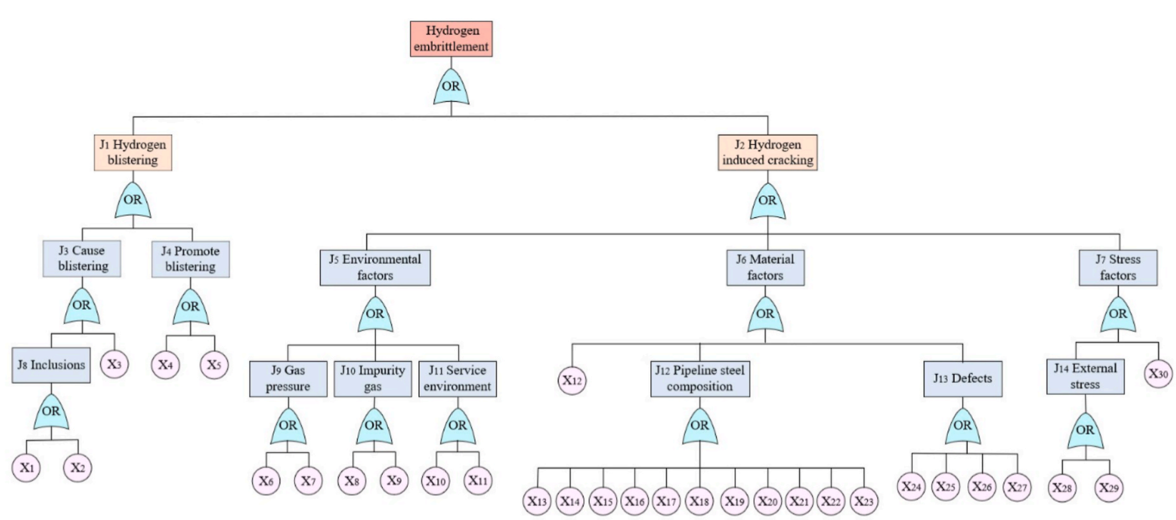

Fig. 4. FTA model for HE.

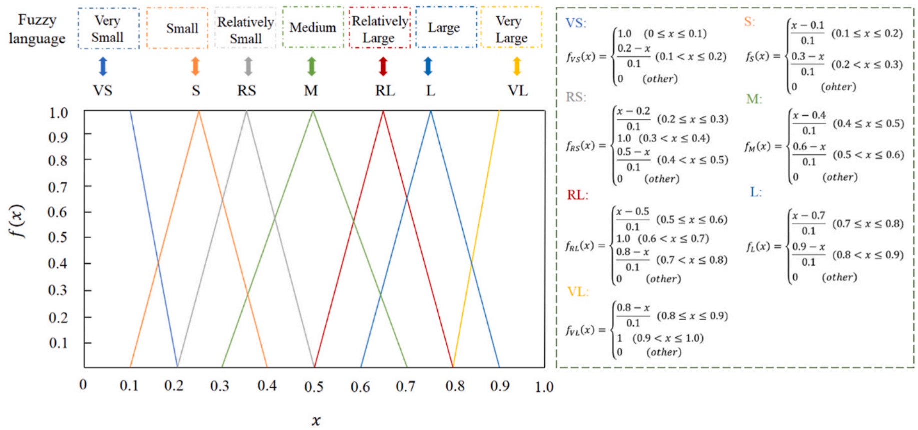

Fig. 5. Fuzzy numbers that represent expert judgment on natural language.

Table 3
Feature of expert weights.

Feature	Level	Scores
Professional position	Professor/Senior manager	5
	Associate professor/Manager	4
	Assistant professor/Assistant manager	3
	Engineer, supervisors	2
	Operator	1
Experience	> 30 years	5
	20–30 years	4
	10–20 years	3
	5–10 years	2
	< 5 years	1
Educational background	Ph.D.	5
	M.Sc.	4
	B.Sc.	3
	College student	2
	Secondary school	1

The form of the non-membership function is presented as Eq. (3):

$$\beta_{\widetilde{H}}(x) = s_{\widetilde{H}}(x) \bullet e^{t2\pi\left(\omega_{\beta\widetilde{H}}(x)\right)} \tag{3}$$

where $t = \sqrt{-1}$, $r_{\widetilde{H}}(x)$, $s_{\widetilde{H}}(x)$, $\omega_{\alpha\widetilde{H}}(x)$, and $\omega_{\beta\widetilde{H}}(x)$ are all real-valued functions and are within [0,1]. Therefore, $r_{\widetilde{H}}(x)+s_{\widetilde{H}}(x) \in [0,1]$ and $\omega_{\alpha\widetilde{H}}(x) + \omega_{\beta\widetilde{H}}(x) \in [0,1]$.

Let $\mathbb{CI}\mathscr{F}^*(U)$ denote the collection of all complex intuitionistic fuzzy sets on universe U. Thus, a complex intuitionistic fuzzy set $\widetilde{H}$ can be represented as a set of ordered pairs, which is presented as Eq. (4):

$$\widetilde{H} = \{\langle x, \alpha_{\widetilde{H}}(x), \beta_{\widetilde{H}}(x)\rangle : x \in U\} \tag{4}$$

where $\alpha_{\widetilde{H}}(x) : U \rightarrow \{h | h \in C, \ |h| \le 1\}$, $\beta_{\widetilde{H}}(x) : U \rightarrow \{h' | h' \in C, \ |h'| \le 1\}$, $|\alpha_{\widetilde{H}}(x) + \beta_{\widetilde{H}}(x)| \le 1$.

D3: Suppose there is an element x in universe U. The complex intuitionistic fuzzy set $\widetilde{H}$ on U can be denoted as $((r_{\widetilde{H}}, \omega_{\alpha\widetilde{H}}), (s_{\widetilde{H}}, \omega_{\beta\widetilde{H}}))$, which is referred to as a complex intuitionistic fuzzy number. The equation about $\widetilde{H}_1$ is presented as Eq. (5):

$$S\left(\widetilde{H}_1\right) = r_{\widetilde{H}_1} - s_{\widetilde{H}_1} + \omega_{\alpha\widetilde{H}_1} - \omega_{\beta\widetilde{H}_1} \tag{5}$$

According to Definition1, 2 and 3, the weight of each expert can be determined by following steps.

(1) **Calculate the score matrix.** According to Eq. (5), the score matrix of $\Re^{(k)} = (\widetilde{h}_{ij}^{(k)})_{n\times n}(k = 1, 2, \cdots, m)$ can be determined by Eq. (6):

$$S^{(k)} = \left(S\left(\widetilde{h}_{ij}^{(k)}\right)\right)_{n\times n} \tag{6}$$

where $\Re$ denotes complex intuitionistic fuzzy preference relations.

(2) **Develop a mean score matrix.** The use of the score function value $f_{ij} = \frac{1}{m}\sum_{k=1}^{m} S(\widetilde{h}_{ij}^{(k)})(i, j = 1, 2, \cdots, n)$ develops the mean score matrix of $S^{(k)} = (S(\widetilde{h}_{ij}^{(k)}))_{n\times n}$. $\overline{S}$ can be determined by Eq. (7):

$$\overline{S} = (f_{ij})_{n\times n} \tag{7}$$

(3) **Determine expert weights.** Using mean deviation analysis equation $H_k = \frac{1}{n^2}\sum_{i=1}^{n}\sum_{j=1}^{n}\left|S(\widetilde{h}_{ij}^{(k)})\right|$, and the expert weights ω_k can be determined by Eq. (8):

$$\omega_k = \frac{1 - H_k}{\sum_{k=1}^{m}(1 - H_k)}, k = 1, 2, \cdots, m \tag{8}$$

where $i, j = 1, 2, \cdots n$; $0 \le \omega_k < 1$ and $\sum_{k=1}^{m}\omega_k = 1$.

3.2.2. *Step 2.2: fuzzification*

FST is employed to process natural language expressions provided by the experts during the judgment process. The natural language-based evaluation values are converted into fuzzy numbers using triangular or trapezoidal fuzzy numbers, enabling a quantitative representation of the linguistic assessments. Fig. 5 illustrates converting natural language expressions into fuzzy numbers using triangular or trapezoidal fuzzy numbers. These fuzzy numbers capture the uncertainty and ambiguity inherent in the linguistic evaluations provided by the experts. By representing the linguistic assessments as fuzzy numbers, the quantitative characteristics of the assessments can be captured, allowing for further analysis and computation within the fuzzy set framework. The choice of triangular or trapezoidal fuzzy numbers depends on the nature of linguistic evaluations and their degree of uncertainties. Triangular fuzzy numbers are characterized by three parameters, representing the lower limit, modal value, and upper limit of the linguistic expression. Trapezoidal fuzzy numbers have four parameters representing the lower limit, left shoulder, right shoulder, and upper limit of the linguistic expression.

For the seven membership functions shown in Fig. 5, each trapezoidal fuzzy number could be represented by (a, b, c, d). It could be determined using the following linear opinion pool to aggregate all the ratings for each BE (Cheliyan and Bhattacharyya, 2018). By incorporating the area defuzzification method, the linear opinion pool can be presented as Eq. (9):

$$M_i = \frac{1}{N_e}\sum_{k=1}^{N_e} A_{ik}\omega_k (i = 1, 2, \cdots, N) \tag{9}$$

where N and N_e denote the number of BEs and experts, respectively; ω_k is the weight of expert k; A_{ik} denotes the linguistic expression (a, b, c, or d) provided by the k-th expert for the i-th BE; and M_i represents the trapezoidal fuzzy number obtained by aggregating all the BEs X_i.

3.2.3. Step 2.3: defuzzification

The use of the Left-Right fuzzy ranking method (Chen and Hwang, 1992) to convert fuzzy numbers to fuzzy possibility scores (FPS) is done by Eqs. (10)–(12):

$$FPS_L = \frac{1-a}{1+b-a} \tag{10}$$

$$FPS_R = \frac{d}{1+d-c} \tag{11}$$

Then,

$$\text{FPS} = \frac{FPS_R + 1 - FPS_L}{2} \tag{12}$$

Convert FPS to fuzzy failure probability $\text{P}(X_i)$ by Eq. (13):

$$\text{P}(X_i) = \begin{cases} \frac{1}{10^k} & (FPS \neq 0) \\ 0 & (FPS = 0) \end{cases} \tag{13}$$

where $k = 2.301 \times \left(\frac{1-FPS}{FPS}\right)^{1/3}$.

3.3. Step 3: correlation of events and estimation of their probability

Quantitative FTA should consider the correlation between events, but they are usually assumed to be mutually independent to simplify calculations. Such simplicity may lead to inaccurate results. There can be a positive, negative, or unknown correlation between events. The degree of correlation can be measured using fuzzy linguistic values that indicate strength. By incorporating the definition of the Pearson correlation coefficient, thirteen fuzzy linguistic values were proposed to describe the degree of correlation between events (Shahriar et al., 2012). Fig. 6 illustrates the corresponding ranges of correlation coefficients for each linguistic level. Depending on the clarity of the correlation between events, the solution methods can be categorized as follows.

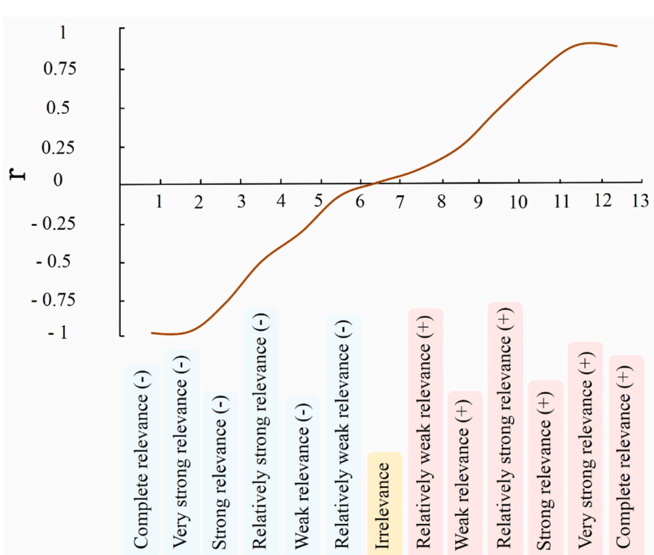

Fig. 6. Correlation coefficients corresponding to different linguistic values.

(1) The probability model of clear correlation of events

According to Fig. 6, the probability of the upper-level event of the correlated events can be estimated by Eqs. (14) and (15) (Frank, 1979):

$$P(X_i \cap X_j) = AND(P_i, P_j, r) = \begin{cases} min(P_i, P_j), r = +1 \\ P_iP_j, r = 0 \\ \max(P_i + P_j - 1, 0), r = -1 \\ log_s\left[1 + \frac{(S^{P_i} - 1)(S^{P_j} - 1)}{s-1}\right], other \end{cases} \tag{14}$$

$$P(X_i \cup X_j) = OR(P_i, P_j, r) = \begin{cases} max(P_i, P_j), r = +1 \\ 1 - (1 - P_i)(1 - P_j), r = 0 \\ \min(P_i + P_j, 1), r = -1 \\ 1 - log_s\left[1 + \frac{(S^{1-P_i} - 1)(S^{1-P_j} - 1)}{s-1}\right], other \end{cases} \tag{15}$$

where $s = tan[\pi(1 - r)/4]$.

(2) The probability model of unclear correlation of events

a) When the degree of correlation between events cannot be determined, but it is known whether they are positively or negatively correlated, the probability of the upper-level event can be calculated by Eqs. (16) and (17):

$$P(X_i \cap X_j) = \begin{cases} AND_+(P_i, P_j) = [P_iP_j, \min(P_i, P_j)] \\ AND_-(P_i, P_j) = [\max(P_i + P_j - 1, 0), P_iP_j] \end{cases} \tag{16}$$

$$P(X_i \cup X_j) = \begin{cases} OR_+(P_i, P_j) = [1 - (1 - P_i)(1 - P_j), \max(P_i, P_j)] \\ OR_-(P_i, P_j) = [1 - (1 - P_i)(1 - P_j), \min(1, P_i + P_j)] \end{cases} \tag{17}$$

b) When the correlation between events cannot be determined, Eqs. (18) and (19) can be used to approximately estimate.

$$P(X_i \cap X_j) = AND(P_i, P_j) = [\max(0, P_i + P_j - 1), \min(P_i, P_j)] \tag{18}$$

$$P(X_i \cup X_j) = OR(P_i, P_j) = [max(P_i, P_j), min(1, P_i + P_j)] \tag{19}$$

3.4. Step 4: estimation of the TE probability

The mentioned method can determine the probabilities of BEs occurring and their correlation. Afterward, the use of the ascending method calculates the failure probability of the TE using the probability models, i.e., Eqs (14)–(19). The calculation process should adhere to the rules of fuzzy algebraic operations (Wolkenhauer, 1997), as shown in Eqs. (20) and (21):

$$P = AND\ F(P_1, P_2, \cdots P_n) = \prod_{i=1}^{n} P_i \quad (i = 1, 2, \ldots, n) \tag{20}$$

$$P = OR\ F(P_1, P_2, \cdots P_n) = 1 - \prod_{i=1}^{n} (1 - P_i) \quad (i = 1, 2, \ldots, n) \tag{21}$$

3.5. Step 5: Risk mitigation

Table 4 shows the recommended ranking of pipeline failure probability in DNV-RP-F107, which can be used to evaluate whether the pipeline risk is acceptable. It is stipulated that the acceptable failure probability is 1×10^{-5}. Maintenance measures to reduce risk must be taken when the failure probability exceeds the threshold.

Table 4
Failure probability ranking for one pipeline in DNV-RP-F107.

Rank	Description	Value
1	It is extremely low frequency that the event is considered negligible.	$< 10^{-5}$
2	The probability of the event is low.	10^{-5}-10^{-4}
3	Events individually are not expected to happen, but when summarized over many pipelines, they have the credibility to happen once a year.	10^{-4}-10^{-3}
4	Individual events may be expected to occur during the life cycle (Typically a 100-year storm).	10^{-3}-10^{-2}
5	Events individually may be expected to occur more than once during the life cycle.	$> 10^{-2}$

4. Case study

A BHNG pipeline segment has been selected for the case study in this work. The pipeline segment has the following specifications: a length of 12 km, a steel grade of API 5L X70, a diameter of 1016 mm, a wall thickness of 14.6 mm, a design pressure of 10 MPa, and a hydrogen blending ratio of 10%. The implementation of the proposed method is followed by the steps in Fig. 3.

4.1. Development of FTA model

The failure analysis of this pipeline segment is conducted using a FTA model, as depicted in Fig. 7. The developed FTA model encompasses a total of 45 BEs. These BEs are derived by connecting the factors contributing to the natural gas pipeline failure with those associated with HE. The connections between these influence factors can be developed using OR gates, indicating that the occurrence of any one of these factors can lead to the BHNG pipeline failure. In addition to HE, Natural disasters and corrosion are identified as the primary hazards for the case pipeline. Table 5 lists the BEs related to these factors (Badida et al., 2019). It should be noted that such BEs could directly or indirectly affect pipeline security.

4.2. Implement of the proposed method

4.2.1. Determining occurrence probability of BEs

A panel of ten experts from various fields, including pipeline engineering, material engineering, structural engineering, and geotechnical engineering, was assembled to assess the probabilities of occurrence for the BEs in the FTA model. The experts' expertise levels and differences were considered by assigning weights to each expert, as determined by Eqs. (1)–(8). The results are presented in Table 6. The experts assessed the probabilities of occurrence for the BEs in the FTA model through a questionnaire and their experience and knowledge from respective fields. The semantic evaluations of all BEs by the ten experts are provided in Table 7. It is worth noting that the evaluation should depend on the situation. Using Eqs. (9)–(13) and the membership function expressions in Fig. 5, the aggregated fuzzy numbers, FPS, and failure probabilities $P(X_i)$ for all the BEs were determined and are presented in Table 8. These values represent the quantification of the probabilities of occurrence for each BE in the FTA model.

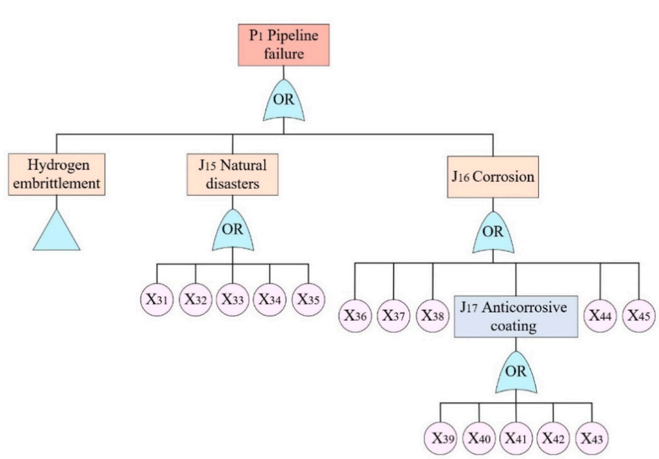

Fig. 7. The FTA model for the case BHNG pipeline.

Table 5
BEs of natural disasters and corrosion (Badida et al., 2019).

BE	Description	BE	Description
X_{31}	Earthquake	X_{39}	High brittleness of anti-corrosion coating
X_{32}	Storm	X_{40}	Aging and peeling of anti-corrosion coating
X_{33}	Landslides	X_{41}	Accumulation of water under the anti-corrosion coating
X_{34}	Floods	X_{42}	Damaged anti-corrosion coating
X_{35}	Lightning	X_{43}	Low adhesion of the anti-corrosion coating
X_{36}	High content of SRB	X_{44}	Low corrosion resistance of pipe steel
X_{37}	Low soil resistivity	X_{45}	High salt content
X_{38}	High content of soil microbial	–	–

Table 6
Features of each expert and their weights.

NO.	Professional position	Experience (year)	Educational background	**Weight (ω_k)**	Rank
1	Professor	32	Ph.D.	0.1198	2
2	Senior manager	33	Ph.D.	0.1205	1
3	Associate professor	28	M.Sc.	0.1065	4
4	Manager	25	M.Sc.	0.1094	3
5	Assistant professor	15	B.Sc.	0.0952	5
6	Assistant manager	17	B.Sc.	0.0947	6
7	Assistant professor	7	College	0.0894	8
8	Supervisor	6	College	0.0899	7
9	Operator	2	Secondary school	0.0869	10
10	Engineer	4	Secondary school	0.0877	9

4.2.2. Determination of correlation probability

Table 9 presents the degree of correlation between the BEs in the FTA model. The correlation between events can have a positive, negative, or unknown effect on their probabilities of occurrence. The degree of correlation is quantified using fuzzy linguistic values, indicating the strength of the correlation. From Table 9, the occurrence probability for the IEs can be calculated using Eqs. (14)–(19). The IEs represent the outcomes of the logical gates connecting the BEs in the FTA model. Table 10 shows the calculated occurrence probabilities of the IEs obtained using the defined probability models and the correlation information from Table 9. These probabilities provide insights into the likelihood of the IEs occurring within the FTA model.

4.2.3. Determination of failure probability of TE

The ascending method is utilized to determine the failure probability of the case BHNG pipeline, resulting in a value of 5.767×10^{-5}. This method involves sequentially calculating the probabilities of occurrence for the BEs in the FTA model, considering their correlations, and applying the defined probability models. In addition, according to Table 4, the value exceeds the acceptable risk rank, so measures to reduce the risk need to be taken.

Table 7
Experts' semantic evaluation value of BEs.

BE/NO.	1	2	3	4	5	6	7	8	9	10
X_1	M	S	S	S	VS	VS	VS	VS	S	VS
X_2	M	S	S	S	RS	RS	S	M	M	RS
X_3	RL	RL	VL	M	VL	VL	L	RL	RL	VL
X_4	S	RS	VS	M	VS	S	RS	RS	M	M
X_5	S	VS	VS	VS	RS	RS	S	VS	S	S
X_6	L	RL	VL	L	L	RL	L	RL	L	L
X_7	L	RL	VL	RL	M	VL	RL	M	RL	L
X_8	L	L	RL	L	VL	L	L	VL	RL	L
X_9	VS	RS	VS	S	RS	M	RS	S	M	M
X_{10}	S	VS	VS	S	S	M	S	M	RS	VS
X_{11}	S	RS	S	S	RS	RS	RS	S	VS	VS
X_{12}	S	VS	RS	RS	M	S	S	RS	S	VS
X_{13}	M	M	S	S	M	M	RS	RS	S	M
X_{14}	S	M	RS	S	M	M	M	RS	RS	S
X_{15}	M	M	RS	RS	M	M	M	S	RS	RS
X_{16}	VS	S	S	S	RS	M	S	RS	M	M
X_{17}	S	RS	RS	RS	M	S	S	M	RS	RS
X_{18}	M	M	M	RS	RS	M	RS	S	RS	S
X_{19}	S	M	RS	S	M	M	M	RS	RS	S
X_{20}	RS	RS	S	VS	S	RS	VS	RS	VS	RS
X_{21}	RS	RS	RS	M	RS	S	S	RS	M	RS
X_{22}	M	RS	RS	M	RS	RS	M	M	RS	RS
X_{23}	S	M	RS	S	M	S	M	RS	RS	S
X_{24}	RS	VS	VS	S	VS	VS	M	VS	RS	RS
X_{25}	RL	RL	RL	M	M	M	RL	RL	RL	M
X_{26}	L	L	RL	M	RL	RL	M	RL	M	RL
X_{27}	RS	RS	S	VS	S	RS	VS	RS	VS	RS
X_{28}	M	M	M	RL	RL	M	RL	M	RL	M
X_{29}	L	L	RL	RL	RL	RL	RL	RL	L	RL
X_{30}	S	VS	VS	VS	RS	RS	S	VS	S	S
X_{31}	L	L	L	RL	RL	RL	L	RL	L	M
X_{32}	RL	L	L	L	L	RL	RL	VL	L	L
X_{33}	M	M	L	RL	RL	L	L	L	M	L
X_{34}	S	S	S	RS	RS	S	RS	RS	S	RS
X_{35}	RL	RL	RL	L	L	L	L	RL	M	M
X_{36}	S	RS	RS	M	M	RS	S	RS	VS	S
X_{37}	RS	RS	S	VS	S	RS	VS	RS	VS	RS
X_{38}	M	M	M	RL	RL	RL	L	M	M	M
X_{39}	S	S	S	S	M	M	RS	VS	RS	S
X_{40}	S	VS	RS	RS	M	S	S	RS	S	VS
X_{41}	M	RS	RS	RS	M	M	M	S	RS	RS
X_{42}	VS	S	S	S	RS	M	S	RS	M	M
X_{43}	S	RS	RS	RS	M	S	S	M	RS	RS
X_{44}	RS	S	M	VS	M	VS	RS	VS	VS	M
X_{45}	S	VS	M	VS	S	VS	RS	M	M	M

Table 8
Calculation results of all BEs.

BE	Aggregated fuzzy number M (a, b, c, and d)	FPS	$P(X_i)$	Rank
X_1	0.00783, 0.01326, 0.02446, 0.03446	0.02365	0.00000001	33
X_2	0.01871, 0.02871, 0.04167, 0.05167	0.03979	0.00000022	22
X_3	0.06023, 0.07023, 0.08132, 0.08748	0.07824	0.00000581	2
X_4	0.01666, 0.02464, 0.03748, 0.04748	0.03573	0.00000013	25
X_5	0.00764, 0.01337, 0.02337, 0.03337	0.02317	0.00000001	33
X_6	0.05808, 0.06908, 0.07908, 0.08801	0.07778	0.00000566	3
X_7	0.05441, 0.06441, 0.07626, 0.08425	0.07368	0.00000446	5
X_8	0.06177, 0.07177, 0.08177, 0.08992	0.08013	0.00000644	1
X_9	0.01617, 0.02391, 0.03660, 0.04660	0.03493	0.00000011	26
X_{10}	0.01141, 0.01827, 0.03011, 0.04011	0.02893	0.00000004	31
X_{11}	0.01225, 0.02051, 0.03051, 0.04051	0.03023	0.00000005	30
X_{12}	0.01288, 0.02080, 0.03175, 0.04175	0.03099	0.00000006	29
X_{13}	0.02215, 0.03215, 0.04733, 0.05733	0.04430	0.00000039	18
X_{14}	0.02083, 0.03083, 0.04483, 0.05483	0.04241	0.00000031	19
X_{15}	0.02430, 0.03430, 0.04950, 0.05950	0.04644	0.00000050	14
X_{16}	0.01604, 0.02484, 0.03753, 0.04753	0.03584	0.00000013	25
X_{17}	0.01881, 0.02881, 0.04066, 0.05066	0.03934	0.00000021	23
X_{18}	0.02264, 0.03264, 0.04705, 0.05705	0.04440	0.00000040	17
X_{19}	0.02083, 0.03083, 0.04483, 0.05483	0.04241	0.00000031	19
X_{20}	0.01227, 0.01941, 0.02941, 0.03941	0.02915	0.00000004	31
X_{21}	0.02012, 0.03012, 0.04209, 0.05209	0.04070	0.00000025	20
X_{22}	0.02409, 0.03409, 0.04817, 0.05817	0.04567	0.00000046	15
X_{23}	0.01894, 0.02894, 0.04199, 0.05199	0.04006	0.00000023	21
X_{24}	0.00966, 0.01460, 0.02549, 0.03549	0.02483	0.00000002	32
X_{25}	0.04226, 0.05226, 0.06613, 0.07613	0.06356	0.00000229	11
X_{26}	0.04669, 0.05669, 0.06955, 0.07955	0.06745	0.00000300	10
X_{27}	0.01227, 0.01941, 0.02941, 0.03941	0.02915	0.00000004	31
X_{28}	0.03762, 0.04762, 0.06381, 0.07381	0.06011	0.00000176	13
X_{29}	0.05327, 0.06327, 0.07327, 0.08327	0.07254	0.00000417	7
X_{30}	0.00764, 0.01337, 0.02337, 0.03337	0.02317	0.00000001	33
X_{31}	0.05348, 0.06348, 0.07435, 0.08435	0.07318	0.00000433	6
X_{32}	0.05876, 0.06876, 0.07876, 0.08786	0.07757	0.00000560	4
X_{33}	0.04814, 0.05814, 0.07141, 0.08141	0.06908	0.00000335	9
X_{34}	0.01472, 0.02472, 0.03472, 0.04472	0.03438	0.00000010	27
X_{35}	0.05040, 0.06040, 0.07214, 0.08214	0.07056	0.00000368	8
X_{36}	0.01734, 0.02647, 0.03852, 0.04852	0.03714	0.00000015	24
X_{37}	0.01227, 0.01941, 0.02941, 0.03941	0.02915	0.00000004	31
X_{38}	0.03867, 0.04867, 0.06478, 0.07478	0.06111	0.00000190	12
X_{39}	0.01466, 0.02376, 0.03566, 0.04566	0.03438	0.00000010	27
X_{40}	0.01288, 0.02080, 0.03175, 0.04175	0.03099	0.00000006	29
X_{41}	0.02309, 0.03309, 0.04708, 0.05708	0.04464	0.00000041	16
X_{42}	0.01604, 0.02484, 0.03753, 0.04753	0.03584	0.00000013	25
X_{43}	0.01881, 0.02881, 0.04066, 0.05066	0.03934	0.00000021	23
X_{44}	0.01407, 0.02026, 0.03316, 0.04316	0.03143	0.00000006	29
X_{45}	0.01507, 0.02182, 0.03553, 0.04553	0.03338	0.00000009	28

4.2.4. *Risk mitigation*

Fig. 8 shows the failure probabilities of the BEs in this case study. The bars colored in red indicate the BEs with relatively high failure probabilities. It can be observed that the primary contribution to pipeline failure is attributed to the high content of H_2S, followed by high hydrogen concentration and high gas pressure. For example, safety protection measures can be implemented from pipeline structure and external measures regarding the high content of H_2S. Structurally, optimizing the process and pipeline design to reduce impurity content and residual stress is possible. Hydrogen barrier coatings can be added to the inner surface of the pipeline to reduce the probability of hydrogen atoms entering the pipeline steel. However, most BHNG pipeline projects are mainly based on existing natural gas pipelines. It is hard to adjust the design of pipeline systems. Thus, more emphasis should be placed on improving external measures. Unlike natural disasters, the pipeline will not immediately fail when detecting HE. However, serious consequences may occur without taking measures. Therefore, pipeline risk can be mitigated through monitoring or maintenance measures when risk probability exceeds the acceptable risk criteria. In terms of detection and inspection, the accuracy of the examination should be improved to capture any signs of HE (Kažys et al., 2022). The maintenance of pipelines can be achieved by increasing safety barriers, which can be achieved by strengthening emergency response policies and optimizing repair and maintenance costs (Yuan et al., 2022). Pipelines should be regularly cleaned to help remove impurities that promote HE (Cauwels et al., 2022). After estimating the failure probability, adopting multiple strategies to reduce the high contribution factor to HE damages to pipelines is crucial, precisely the contribution of this work.

4.3. *Discussion*

The proposed method was employed to estimate the failure probability of a natural gas pipeline to quantify the additional risks brought by mixed hydrogen transportation. A FTA model for the natural gas pipeline was constructed, as depicted in Fig. 9, and the corresponding BEs were identified and listed in Table 4 (Badida et al., 2019). An expert group provided semantic evaluations for the BEs, as presented in Table 7. Table 11 showcases the aggregated fuzzy numbers *M*, fuzzy possibility values FPS, and failure probabilities $P(X_i)$ associated with the BEs. Furthermore, Table 12 illustrates the correlations between the events. By utilizing the correlation probability model and the ascending method, the failure probability of the pipeline (referred to as P_2) was determined to be 2.019×10^{-5}. Fig. 10 compares the failure probabilities for the same natural gas pipeline with and without hydrogen injection. It is clear that the introduction of hydrogen dramatically increases the likelihood of failure, which is found to be 2.856 times

Table 9
Correlation of events in the FTA model.

NO.	Intermediate events	Related events	Logical gate	Correlation degree	r	Probability model
J_9	Gas pressure	X_6, X_7	OR	Relatively strong relevance (+)	$r = 0.5$	Eq. (22)
J_{10}	Impurity gas	X_8, X_9	OR	Unknown relevance	–	Eq. (26)
J_{14}	External stress	X_{28}, X_{29}	OR	Relatively strong relevance (+)	$r = 0.5$	Eq. (22)
J_{15}	Natural disasters	X_{33}, X_{34}	OR	Relatively strong relevance (+)	$r = 0.5$	Eq. (22)
J_{17}	Anticorrosive coating	X_{39}, X_{40}	OR	(+)	–	Eq. (24)
Others			AND	Irrelevance	$r = 0$	Eq. (21)
			OR	Irrelevance	$r = 0$	Eq. (22)

Table 10
Failure probabilities of intermediate events (J_i).

NO.	Intermediate events	Probability	NO.	Intermediate events	Probability
J_1	Hydrogen blistering	0.00000618	**J_{10}**	Impurity gas	0.00000651
J_2	Hydrogen induced cracking	0.00003130	**J_{11}**	Service environment	0.00000009
J_3	Blistering initiation	0.00000604	**J_{12}**	Pipeline steel composition	0.00000323
J_4	Blistering propagation	0.00000014	**J_{13}**	Defects	0.00000535
J_5	Environmental factors	0.00001672	**J_{14}**	External stress	0.00000593
J_6	Material factors	0.00000864	**J_{15}**	Natural disasters	0.00001706
J_7	Stress factors	0.00000594	**J_{16}**	Corrosion	0.00000313
J_8	Inclusions	0.00000023	**J_{17}**	Anticorrosive coating	0.00000089
J_9	Gas pressure	0.00001012	–	–	–

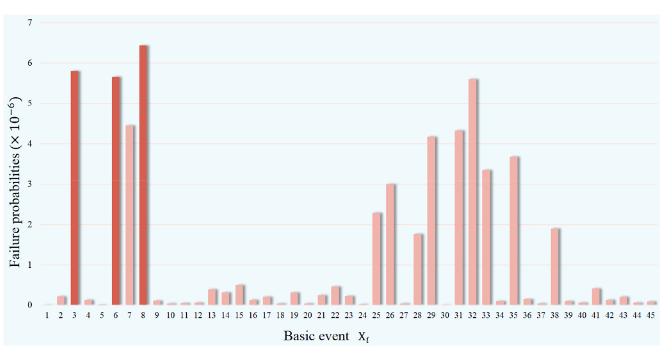

Fig. 8. Failure probability of each BE.

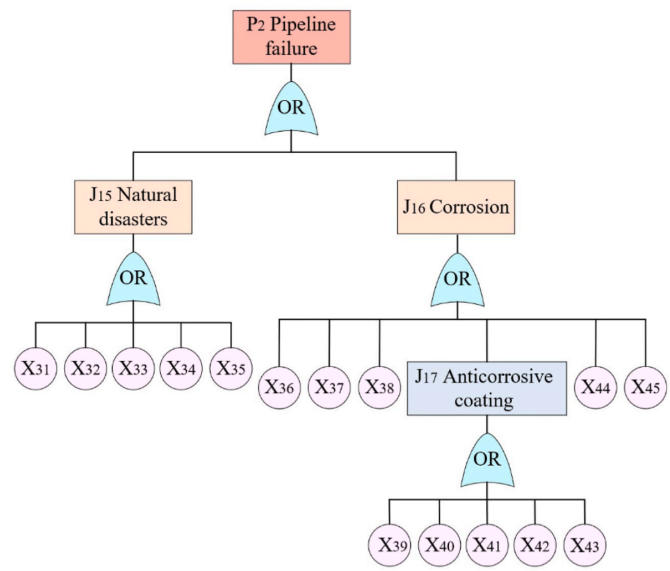

Fig. 9. The FTA model of the natural gas pipeline.

Table 11
List of BEs in FTA model for the case natural gas pipeline.

BE	Aggregated fuzzy number M (a, b, c and d)	FPS	$P(X_i)$	Rank
X_{31}	0.05348, 0.06348, 0.07435, 0.08435	0.07318	0.00000433	2
X_{32}	0.05876, 0.06876, 0.07876, 0.08786	0.07757	0.00000560	1
X_{33}	0.04814, 0.05814, 0.07141, 0.08141	0.06908	0.00000335	4
X_{34}	0.01472, 0.02472, 0.03472, 0.04472	0.03438	0.00000010	10
X_{35}	0.05040, 0.06040, 0.07214, 0.08214	0.07056	0.00000368	3
X_{36}	0.01734, 0.02647, 0.03852, 0.04852	0.03714	0.00000015	8
X_{37}	0.01227, 0.01941, 0.02941, 0.03941	0.02915	0.00000004	13
X_{38}	0.03867, 0.04867, 0.06478, 0.07478	0.06111	0.00000190	5
X_{39}	0.01466, 0.02376, 0.03566, 0.04566	0.03438	0.00000010	10
X_{40}	0.01288, 0.02080, 0.03175, 0.04175	0.03099	0.00000006	12
X_{41}	0.02309, 0.03309, 0.04708, 0.05708	0.04464	0.00000041	6
X_{42}	0.01604, 0.02484, 0.03753, 0.04753	0.03584	0.00000013	9
X_{43}	0.01881, 0.02881, 0.04066, 0.05066	0.03934	0.00000021	7
X_{44}	0.01407, 0.02026, 0.03316, 0.04316	0.03143	0.00000006	12
X_{45}	0.01507, 0.02182, 0.03553, 0.04553	0.03338	0.00000009	11

higher compared to when hydrogen is not present. This is primarily due to the additional risks introduced by hydrogen.

This work demonstrates that blending hydrogen into an existing natural gas pipeline substantially increases the failure probability compared to when hydrogen is not present. Therefore, risk assessment and mitigation strategies are needed when transporting hydrogen into in-service natural gas pipelines or developing new hydrogen transportation infrastructure. The additional risks associated with hydrogen damage, such as HIC and HB, should be accurately analyzed and controlled to guarantee the integrity and safety of the pipeline. This work highlights the importance of considering correlations between various influence factors in the pipeline system. Understanding these interdependencies allows for a more comprehensive and accurate assessment of the failure probability. As the energy sector explores the integration of hydrogen as a cleaner energy source, it is crucial to assess the potential impacts on existing infrastructure (Cheng and Cheng, 2023). The present study helps decision-makers, pipeline operators, and engineers understand the HE. It underscores the importance of proactive risk management and considering additional risks when introducing hydrogen into existing infrastructure, thus contributing to the safe and reliable deployment of hydrogen as an energy carrier.

5. Conclusions and limitations

The present study proposed a flexible method to quantitatively estimate the failure probability of pipelines due to HE. An indicator system of HIC and HB was developed regarding the thermodynamic conditions of HE, permeation and diffusion behavior of hydrogen, and failure mechanisms. A FTA model of HE, including HIC and HB, was developed by mapping the developed indicator system and capturing the logical relationship between the events. The FTA model of the BHNG pipeline

Table 12
Correlations of events in the FTA model of the case natural gas pipeline.

NO.	Intermediate events	Events	Logical gate	Correlation degree	r	Probability model
J_{15}	Natural disasters	X_{33}, X_{34}	OR	Relatively strong relevance (+)	$r = 0.5$	Eq. (22)
J_{17}	Anticorrosive coating	X_{39}, X_{40}	OR	(+)	–	Eq. (24)
Others			AND	Irrelevance	$r = 0$	Eq. (21)
			OR	Irrelevance	$r = 0$	Eq. (22)

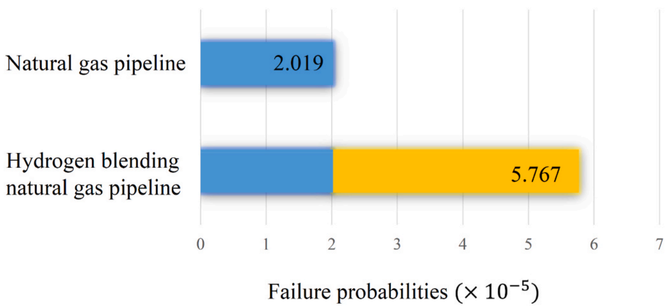

Fig. 10. Failure probability of natural gas pipeline and BHNG pipeline.

was constructed by correlating the HE with the conventional failure factors of the natural gas pipeline using the OR gate. By considering the correlations between events, the failure probability of a BHNG pipeline was estimated using a hybrid method. Through a case study, it was observed that the failure probability of the case natural gas pipeline significantly increases after blending hydrogen, reaching a value 2.856 times higher than that of the corresponding natural gas pipeline. Among the contributing BEs, the highest contribution to the failure probability was attributed to the high content of H_2S, followed by high hydrogen concentration and high gas pressure. This study also introduced maintenance measures to mitigate risks regarding the high content of H_2S.

The proposed IFFTA method and risk reduction measures hold significant importance in assisting pipeline operators in understanding better the suitability and potential risks associated with transporting hydrogen in natural gas pipelines. The proposed measures to reduce risks can provide a significant reference value for operators. Operators can make informed decisions regarding safe and efficient hydrogen transportation by quantifying the failure probability. This method enables proactive measures to be taken for pipeline integrity management and supports the development of guidelines and regulations for hydrogen transportation in existing natural gas infrastructure. While the proposed method can be utilized to estimate the failure probability of BHNG pipelines for scenarios with limited or unavailable quantitative data, exploring and developing advanced quantitative methods to address these limitations is crucial. Operational data should be used to verify the fuzzy comprehensive evaluation results as well. In the future, graph theory such as Bayesian network-based method can be developed to capture the complex interaction between influencing factors.

CRediT authorship contribution statement

Guojin Qin: Writing – original draft, Methodology, Investigation, Funding acquisition, Formal analysis, Conceptualization. **Ruiling Li:** Writing – original draft, Visualization, Methodology, Investigation, Data curation. **Ming Yang:** Writing – review & editing. **Bohong Wang:** Writing – review & editing. **Pingan Ni:** Visualization, Validation, Data curation. **Yihuan Wang:** Writing – review & editing, Supervision, Project administration, Funding acquisition.

Declaration of competing interest

None.

Data availability

Data will be made available on request.

Acknowledgment

The authors would like to acknowledge all the financial support, including Southwest Petroleum University (NO. 2022QHZ016; NO. 202299010028), China Postdoctoral Science Foundation (NO. 2023M742287) and National Natural Science Foundation of China (52304258; 52302420).

References

Adumene, S., Khan, F., Adedigba, S., Zendehboudi, S., 2021a. Offshore system safety and reliability considering microbial influenced multiple failure modes and their interdependencies. Reliab. Eng. Syst. Saf. 215, 107862.
Adumene, S., Khan, F., Adedigba, S., Zendehboudi, S., Shiri, H., 2021b. Dynamic Risk Analysis of Marine and Offshore Systems Suffering Microbial Induced Stochastic Degradation, vol. 207. Reliability Engineering & System Safety, 107388.
Adumene, S., Khan, F., Adedigba, S., 2020. Operational safety assessment of offshore pipeline with multiple MIC defects. Comput. Chem. Eng. 138, 106819.
Ali, K., Qin, J., Faber, M.H., 2022. On information modeling in structural integrity management. Struct. Health Monit. 21, 59–71.
Arena, S., Manca, G., Murru, S., Orrù, P.F., Perna, R., Reforgiato Recupero, D., 2022. Data science application for failure data management and failure prediction in the oil and gas industry: a case study. Appl. Sci. 12 (20), 10617.
Badida, P., Balasubramaniam, Y., Jayaprakash, J., 2019. Risk evaluation of oil and natural gas pipelines due to natural hazards using fuzzy fault tree analysis. J. Nat. Gas Sci. Eng. 66, 284–292.
Cauwels, M., Depraetere, R., De Waele, W., Hertelé, S., Depover, T., Verbeken, K., 2022. Influence of electrochemical hydrogenation parameters on microstructures prone to hydrogen-induced cracking. J. Nat. Gas Sci. Eng. 101, 104533.
Cheliyan, A.S., Bhattacharyya, S.K., 2018. Fuzzy fault tree analysis of oil and gas leakage in subsea production systems. J. Ocean Eng. Sci. 3 (1), 38–48.
Chen, C., Li, C., Reniers, G., Yang, F., 2021. Safety and security of oil and gas pipeline transportation: a systematic analysis of research trends and future needs using WoS. J. Clean. Prod. 279, 123583.
Chen, S.J., Hwang, C.L., 1992. Fuzzy Multiple Attribute Decision Making Methods. Springer Berlin Heidelberg, pp. 289–486.
Cheng, W., Cheng, Y.F., 2023. A techno-economic study of the strategy for hydrogen transport by pipelines in Canada. J. Pipeline Sci. Eng., 100112
Cheng, Y.F., 2023. Essence and gap analysis for hydrogen embrittlement of pipelines in high-pressure hydrogen environments. Oil Gas Storage Transp. 42 (1), 1–8.
Cheng, Y.F., 2022. Hydrogen Transport in Aged Pipelines II. Technical Assessment of the Susceptibility to Hydrogen Embrittlement. AMPP/ASM International Calgary Chapter Luncheon, Calgary. Canada.
Cui, J., Aziz, M., 2023. Techno-economic analysis of hydrogen transportation infrastructure using ammonia and methanol. Int. J. Hydrogen Energy 48 (42), 15737–15747.
Dahire, S., Tahir, F., Jiao, Y., Liu, Y., 2018. Bayesian Network inference for probabilistic strength estimation of aging pipeline systems. Int. J. Pres. Ves. Pip. 162, 30–39.
Dundulis, G., Žutautaitė, I., Janulionis, R., Ušpuras, E., Rimkevičius, S., Eid, M., 2016. Integrated failure probability estimation based on structural integrity analysis and failure data: natural gas pipeline case. Reliab. Eng. Syst. Saf. 156, 195–202.
Dunne, D.P., Hejazi, D., Saleh, A.A., Haq, A.J., Calka, A., Pereloma, E.V., 2016. Investigation of the effect of electrolytic hydrogen charging of X70 steel: I. The effect of microstructure on hydrogen-induced cold cracking and blistering. Int. J. Hydrogen Energy 41 (28), 12411–12423.
Dutta, S., 2014. A review on production, storage of hydrogen and its utilization as an energy resource. J. Ind. Eng. Chem. 20 (4), 1148–1156.
Elaoud, S., Hadj-Taïeb, E., 2008. Transient flow in pipelines of high-pressure hydrogen–natural gas mixtures. Int. J. Hydrogen Energy 33 (18), 4824–4832.
Erdener, B.C., Sergi, B., Guerra, O.J., Chueca, A.L., Pambour, K., Brancucci, C., Hodge, B. M., 2023. A review of technical and regulatory limits for hydrogen blending in natural gas pipelines. Int. J. Hydrogen Energy 48 (14), 5595–5617.
Feng, X., Jiang, J.C., Wang, W.F., 2020. Gas pipeline failure evaluation method based on a Noisy-OR gate bayesian network. J. Loss Prev. Process. Ind. 66, 104175.
Frank, M.J., 1979. On the simultaneous associativity of F (x, y) and x+ y-F (x, y). Aequationes Math. 19, 194–226.

Ge, F., Huang, F., Yuan, W., Peng, Z., Liu, J., Cheng, Y.F., 2020. Effect of tensile stress on the hydrogen permeation of MS X65 pipeline steel under sulfide films. Int. J. Hydrogen Energy 45 (22), 12419–12431.
Girgin, S., Krausmann, E., 2013. RAPID-N: rapid natech risk assessment and mapping framework. J. Loss Prev. Process. Ind. 26 (6), 949–960.
Guo, S., Xu, L., Dong, S., Cheng, Y.F., 2023a. Finite element modeling of hydrogen atom diffusion and distribution at corrosion defect on aged pipelines transporting hydrogen. Int. J. Hydrogen Energy 48 (36), 13566–13577.
Guo, S., Xu, L., Dong, S., Cheng, Y.F., 2023b. Finite element modeling of hydrogen atom diffusion and distribution at corrosion defect on aged pipelines transporting hydrogen. Int. J. Hydrogen Energy 48 (36), 13566–13577.
Han, Y.D., Wang, R.Z., Wang, H., Xu, L.Y., 2019. Hydrogen embrittlement sensitivity of X100 pipeline steel under different pre-strain. Int. J. Hydrogen Energy 44 (39), 22380–22393.
Hong, B., Shao, B., Guo, J., Fu, J., Li, C., Zhu, B., 2023. Dynamic Bayesian network risk probability evolution for third-party damage of natural gas pipelines. Appl. Energy 333, 120620.
Huang, F., Cheng, P., Zhao, X.Y., Liu, J., Hu, Q., Cheng, Y.F., 2017. Effect of sulfide films formed on X65 steel surface on hydrogen permeation in H2S environments. Int. J. Hydrogen Energy 42 (7), 4561–4570.
Huang, S., Hui, H., Peng, J., 2023. Prediction of hydrogen-assisted fracture under coexistence of hydrogen-enhanced plasticity and decohesion. Int. J. Hydrogen Energy 48, 36987–37000.
Huang, Y., Qin, G., Yang, M., 2023. A risk-based approach to inspection planning for pipelines considering the coupling effect of corrosion and dents. Process Saf. Environ. 180, 588–600.
Jia, G., Lei, M., Li, M., Xu, W., Li, R., Lu, Y., Cai, M., 2023. Hydrogen embrittlement in hydrogen-blended natural gas transportation systems: a review. Int. J. Hydrogen Energy 48 (82), 32137–32157.
Jiang, Y., Li, C., Wang, D., Di, X., 2021. Effect of cyclic plastic deformation on hydrogen diffusion behavior and embrittlement susceptibility of reeling-pipeline steel weldments. Int. J. Hydrogen Energy 46 (58), 30158–30172.
Jianxing, Y., Haicheng, C., Yang, Y., Zhenglong, Y., 2019. A weakest t-norm based fuzzy fault tree approach for leakage risk assessment of submarine pipeline. J. Loss Prevent. Proc. 62, 103968.
Kažys, R.J., Mažeika, L., Samaitis, V., Šliteris, R., Merck, P., Viliūnas, Ž., 2022. Comparative analysis of ultrasonic NDT techniques for the detection and characterisation of hydrogen-induced cracking. Materials 15 (13), 4551.
Khan, F., Yarveisy, R., Abbassi, R., 2021. Risk-based pipeline integrity management: a road map for the resilient pipelines. J. Pipeline Sci. Eng. 1 (1), 74–87.
Kim, W.K., Park, G.T., Kim, K.Y., 2021. Stress oriented hydrogen induced cracking of linepipe steel. J. Iron Steel Res. Int. 1.
Lang, F., Huang, F., Yue, J., Li, L., Xu, J., Liu, J., 2023. Hydrogen trapping and hydrogen embrittlement (HE) susceptibility of X70 grade high-strength, acid-resistant, submarine pipeline steel with Mg treatment. J. Mater. Res. Technol. 24, 623–638.
Li, H., Niu, R., Li, W., Lu, H., Cairney, J., Chen, Y.S., 2022a. Hydrogen in pipeline steels: recent advances in characterization and embrittlement mitigation. J. Nat. Gas Sci. Eng. 105, 104709.
Li, Y.T., He, X.N., Shuai, J., 2022b. Risk analysis and maintenance decision making of natural gas pipelines with external corrosion based on Bayesian network. Petrol. Sci. 19 (3), 1250–1261.
Li, Y., Gong, B., Li, X., Deng, C., Wang, D., 2018. Specimen thickness effect on the property of hydrogen embrittlement in single edge notch tension testing of high strength pipeline steel. Int. J. Hydrogen Energy 43 (32), 15575–15585.
Li, Y., Kuang, Z., Fan, Z., Shuai, J., 2023. Evaluation of the safe separation distances of hydrogen-blended natural gas pipelines in a jet fire scenario. Int. J. Hydrogen Energy 48 (49), 18804–18815.
Liu, Z.Y., Li, X.G., Du, C.W., Cheng, Y.F., 2009. Local additional potential model for effect of strain rate on SCC of pipeline steel in an acidic soil solution. Corrosion Sci. 51 (12), 2863–2871.
Mao, L.Y., Luo, Z.A., Huang, C., Zhang, X.M., 2022. Hydrogen embrittlement behavior in interstitial Mn–N austenitic stainless steel. Int. J. Hydrogen Energy 47 (86), 36716–36732.
Martin, M.L., Sofronis, P., 2022. Hydrogen-induced cracking and blistering in steels: a review. J. Nat. Gas Sci. Eng. 101, 104547.
Meng, B., Gu, C., Zhang, L., Zhou, C., Li, X., Zhao, Y., Han, Y., 2017. Hydrogen effects on X80 pipeline steel in high-pressure natural gas/hydrogen mixtures. Int. J. Hydrogen Energy 42 (11), 7404–7412.
Mohtadi-Bonab, M.A., 2022. Effect of different parameters on hydrogen affected fatigue failure in pipeline steels. Eng. Fail. Anal. 137, 106262.
Molavitabrizi, D., Yu, H., Mousavi, S.M., 2022. Hydrogen embrittlement in micro-architectured materials. Eng. Fract. Mech. 274, 108762.
Nguyen, T.T., Tak, N., Park, J., Nahm, S.H., Beak, U.B., 2020. Hydrogen embrittlement susceptibility of X70 pipeline steel weld under a low partial hydrogen environment. Int. J. Hydrogen Energy 45 (43), 23739–23753.
Ohaeri, E., Eduok, U., Szpunar, J., 2018. Hydrogen related degradation in pipeline steel: a review. Int. J. Hydrogen Energy 43 (31), 14584–14617.
Pluvinage, G., Capelle, J., Meliani, M.H., 2019. Pipe networks transporting hydrogen pure or blended with natural gas, design and maintenance. Eng. Fail. Anal. 106, 104164.
Pourazizi, R., Mohtadi-Bonab, M.A., Davani, R.K.Z., Szpunar, J.A., 2021. Effect of thermo-mechanical controlled process on microstructural texture and hydrogen embrittlement resistance of API 5L X70 pipeline steels in sour environments. Int. J. Pres. Ves. Pip. 194, 104491.
Qin, G., Zhang, Z., Hou, X., Lu, H., Huang, Y., Wang, Y., 2023. Condition assessment of underground corroded pipelines subject to hydrogen damage and combined internal pressure and axial compression. Tunn. Undergr. Sp. Tech. 142, 105389.
Ranjbar, M., Miresmaeili, R., Naimi-Jamal, M.R., Mirzaei, M., 2021. Effect of microstructure on the mechanical properties and fracture toughness of API X65 pipeline Steel in the presence of hydrogen. Met. Mater. Int. 27, 3918–3934.
Ren, X., Chu, W., Li, J., Su, Y., Qiao, L., 2008. The effects of inclusions and second phase particles on hydrogen-induced blistering in iron. Mater. Chem. Phys. 107 (2–3), 231–235.
Shah, K.J., Pan, S.Y., Lee, I., Kim, H., You, Z., Zheng, J.M., Chiang, P.C., 2021. Green transportation for sustainability: review of current barriers, strategies, and innovative technologies. J. Clean. Prod. 326, 129392.
Shahriar, A., Sadiq, R., Tesfamariam, S., 2012. Risk analysis for oil & gas pipelines: a sustainability assessment approach using fuzzy based bow-tie analysis. J. Loss Prevent. Proc. 25 (3), 505–523.
Shan, K., Shuai, J., Xu, K., Zheng, W., 2018. Failure probability assessment of gas transmission pipelines based on historical failure-related data and modification factors. J. Nat. Gas Sci. Eng. 52, 356–366.
Silva, S.C., Silva, A.B., Gomes, J.P., 2021. Hydrogen embrittlement of API 5L X65 pipeline steel in CO2 containing low H2S concentration environment. Eng. Fail. Anal. 120, 105081.
Song, L., Liu, Z., Li, X., Du, C., 2020. Characteristics of hydrogen embrittlement in high-pH stress corrosion cracking of X100 pipeline steel in carbonate/bicarbonate solution. Construct. Build. Mater. 263, 120124.
Sun, Y., Cheng, Y.F., 2021a. Thermodynamics of spontaneous dissociation and dissociative adsorption of hydrogen molecules and hydrogen atom adsorption and absorption on steel under pipelining conditions. Int. J. Hydrogen Energy 46 (69), 34469–34486.
Sun, Y., Cheng, Y.F., 2021b. Thermodynamics of spontaneous dissociation and dissociative adsorption of hydrogen molecules and hydrogen atom adsorption and absorption on steel under pipelining conditions. Int. J. Hydrogen Energy 46 (69), 34469–34486.
Sun, Y., Ren, Y., Cheng, Y.F., 2022. Dissociative adsorption of hydrogen and methane molecules at high-angle grain boundaries of pipeline steel studied by density functional theory modeling. Int. J. Hydrogen Energy 47 (97), 41069–41086.
Wang, F., Gong, Z., Shao, Y., 2022a. Incomplete complex intuitionistic fuzzy system: preference relations, expert weight determination, group decision-making and their calculation algorithms. Axioms 11 (8), 418.
Wang, Y., Xia, A., Qin, G., 2022b. Probabilistic modeling for reliability analysis of buried pipelines subjected to spatiotemporal earthquakes. Probabilist. Eng. Mech. 69, 103315.
Wang, Y., Xia, A., Zhang, P., Qin, G., 2022c. Probabilistic physical modeling of randomly corroded surface and its use in reliability analysis of corroded pipelines under spatiotemporal vibration. Ocean Eng. 262, 112219.
Wang, Y., Zhang, Z., Liu, S., Xia, A., Li, R., Qin, G., 2023. Importance sampling-based probabilistic performance modeling of low-, mid-and high-strength pipelines under coupling effect of hydrogen-induced damage and corrosion. Process Saf. Environ. 180, 428–442.
Wang, Y., Zhang, P., Qin, G., 2021. Reliability assessment of pitting corrosion of pipeline under spatiotemporal earthquake including spatial-dependent corrosion growth. Process Saf. Environ. 148, 166–178.
Wolkenhauer, O., 1997. A course in fuzzy systems and control. Int. J. Electr. Eng. Educ. 34 (3), 282.
Wu, X., Zhang, H., Yang, M., Jia, W., Qiu, Y., Lan, L., 2022. From the perspective of new technology of blending hydrogen into natural gas pipelines transmission: mechanism, experimental study, and suggestions for further work of hydrogen embrittlement in high-strength pipeline steels. Int. J. Hydrogen Energy 47 (12), 8071–8090.
Xu, Z., Zhang, P., Zhang, B., Lei, B., Feng, Z., Shao, Y., et al., 2022. Effect of tensile stress on the hydrogen adsorption of X70 pipeline steel. Int. J. Hydrogen Energy 47 (50), 21582–21595.
Yadav, S., Jack, T.A., Davani, R.K.Z., Ohaeri, E., Szpunar, J., 2022. Effect of post-processing heat treatment on hydrogen embrittlement susceptibility of API 5L X70 pipeline steel. Int. J. Pres. Ves. Pip. 199, 104762.
Yazdi, M., Mohammadpour, J., Li, H., Huang, H.Z., Zarei, E., Pirbalouti, R.G., Adumene, S., 2023. Fault tree analysis improvements: a bibliometric analysis and literature review. Qual. Reliab. Eng. Int. 2023, 1–21.
Yen, S.K., Huang, I.B., 2003. Critical hydrogen concentration for hydrogen-induced blistering on AISI 430 stainless steel. Mater. Chem. Phys. 80 (3), 662–666.
Yu, W., Huang, W., Wen, K., Zhang, J., Liu, H., Wang, K., Gong, J., Qu, C., 2021. Subset simulation-based reliability analysis of the corroding natural gas pipeline. Reliab. Eng. Syst. Safe. 213, 107661.
Yuan, S., Yang, M., Reniers, G., Chen, C., Wu, J., 2022. Safety barriers in the chemical process industries: a state-of-the-art review on their classification, assessment, and management. Saf. Sci. 148, 105647.
Zhang, J., Cheng, Y.F., 2023. Study by finite element modeling of hydrogen atom diffusion and distribution at a dent on existing pipelines for hydrogen transport. J. Clean. Prod. 418, 138165.
Zhang, P., Wang, Y., Qin, G., 2018. Fuzzy damage analysis of the seismic response of a long-distance pipeline under a coupling multi-influence domain. Energies 12, 62.
Zhang, S., Zhao, Q., Liu, J., Huang, F., Huang, Y., Li, X., 2019. Understanding the effect of niobium on hydrogen-induced blistering in pipeline steel: a combined experimental and theoretical study. Corrosion Sci. 159, 108142.

Zhao, F., Wang, Z., Dong, B., Li, M., Ji, Y., Han, F., 2023. Comprehensive life cycle cost analysis of ammonia-based hydrogen transportation scenarios for offshore wind energy utilization. J. Clean. Prod. 429, 139616.

Zhou, C., Ye, B., Song, Y., Cui, T., Xu, P., Zhang, L., 2019. Effects of internal hydrogen and surface-absorbed hydrogen on the hydrogen embrittlement of X80 pipeline steel. Int. J. Hydrogen Energy 44 (40), 22547–22558.

Zhou, Q.J., Qiao, L.J., Qi, H.B., Li, J.X., He, J.Y., Chu, W.Y., 2007. Hydrogen blistering and hydrogen-induced cracking in amorphous nickel phosphorus coating. J. Non-Cryst. Solids 353 (44–46), 4011–4014.